



Internship Report

ADVANCED NANO-ENGINEERING TO TRANSPORT HEAT IN ULTRA-THIN MEMBRANES (2D MATERIALS)

Cléophanie Brochard-Richard
Supervisor : Julien Chaste

Université de Paris
Politecnico di Torino

Academic Year 2020/2021

Contents

1	General context	1
1.1	Introduction	1
1.2	Issues	1
1.3	Scientific objectives	2
2	Presentation of the lab and the team	2
3	Presentation of the internship subject	2
3.1	State of the art	2
3.2	Scientific problems to solve	3
3.3	Specificity of the subject	4
3.4	Objectives	4
4	Results	4
4.1	Setup	4
4.2	Use of Raman spectroscopy for sample characterisation	6
4.3	Electrical heating by Joule effect of 2D material on substrate	9
4.4	Electrical heating by Joule effect on suspended 2D materials	11
4.5	Technique of transfer on holes	13
4.6	Technique of transfer on heaters	15
4.7	Thermal measurements on heaters	17
5	Conclusion and perspectives	20

1 General context

1.1 Introduction

In our common life, everything is dependent of heat. The energy that the sun gives us, the one loss due to friction, the one loss by dissipation, the Joule effect. In most of those cases, the energy loss that we had previously is due to the heat dissipation. To avoid this loss of energy in a circuit, we need to use materials that have thermoelectric properties allowing to have low thermal losses even with a high electrical conductivity. That is something very hard to obtain in a bulk sample. However, new materials were discovered with wide and various properties. 2D materials are of them. These materials are synthesized by Chemical Vapor Deposition (CVD) , by epitaxy or can be exfoliated from crystals. 2D materials form planar layers. Those layers do not have the same kind of interaction in in-plane and out of plane directions. There is an anisotropy of the material and that change all the properties of the material. Since they are in two dimensions, new behaviors emerge. The band gap that is indirect in 3D material can become direct in 2D materials. The bonds do not follow the 3D configuration and there are no dangling bonds. That produces high reactivity when this material is in interaction with the environment. In 2D materials, it is possible to have high energy excitons. For example, that is the case in transition metal dichalcogenides (TMD) that are 2D semiconductors. In these materials, various excitons are available [15]. The mechanical properties also diverge from the 3D materials.

Another example of disparity appears with phonons. They do not follow the same behavior in 2D material than in 3D materials. Because of that, the link between thermal conductivity and electrical conductivity may be very different and can overcome the traditional limits. It is promising to study thermal and thermoelectric properties of 2D materials. Indeed, that could help to lower the loss of energy. We could be able to convert heat in electrical energy by Seebeck effect. We can have with that a source of energy those origin is the thermal energy. Since heat is usually the source of energy losses, that solves two problems at the same time. On one hand, there are less energy losses and on the other hand, more energy that we can use. Moreover, the 2D materials exhibit thermal conductivity corresponding to the whole spectrum of thermal conductivity of 3D materials. Indeed, Graphene have a conductivity of about $4000 \text{ W.m}^{-1}.\text{K}^{-1}$ whereas InP_3 have a thermal conductivity around $0.64 \text{ W.m}^{-1}.\text{K}^{-1}$ [18]. That corresponds to the full spectrum that we can achieve with 3D materials.

1.2 Issues

There are great interest to understand thermal and thermoelectric properties of 2D materials. In this work, we will focus our attention on the thermal conductivity. To obtain it, we need to heat our sample. We use 2 methods to investigate this field. First, we realize an electrical circuit with our 2D material as a part of it. It acts as a resistance. The difference of electrical potential between both sides of the material leads to an electrical current flux. That causes an elevation of the material's temperature by Joule effect. It is then possible to study the thermal behavior of the structure. Another setup that we can have consists of an electrical circuit with a resistance that is heated by Joule effect used as a heat source. On the hot part of this circuit, we can put our 2D material. If only a part of the 2D material is on the heater, there is a gradient of temperature through it. In this case, we observe the propagation of the heat inside the 2D material.

We need a tool that allows us to detect the temperature change at a good resolution. For this purpose, we use a micro-Raman spectroscopy that allows us to detect optical phonons in our sample. With this information, we can turn back to the temperature at the point where the laser is focused. This technique is useful since it is a non-destructive technique. We realize measurements and change of the temperature at the same time. 2D materials are fragile materials. Because of that, we can not put them easily on the heaters or on electrical circuits. Since they can not be directly fabricate on those materials, we have to transfer them on the useful substrate. The transfer is an important technique that need to be mastered if we want to study 2D materials.

1.3 Scientific objectives

2D materials do not follow 3D physical laws. It may be useful to understand how do they work. This information can be of interest for applications afterwards in other nano objects. Thermal transport is linked to the propagation of phonons and understand why the phonons acts as they do would allow us to open new perspectives in the world. Moreover, some applications can exploit the discovered properties.

2 Presentation of the lab and the team

The internship was done in the Centre de Nanosciences et de Nanotechnologies (C2N) in Palaiseau. This laboratory is part of the Université Paris Saclay. It is specialized in the elaboration and the characterization of nanomaterials in order to produce devices for nanotechnologies. The department in which I worked was the Material department that elaborates and studies new nanomaterials. It is specialized in the epitaxy growth and others growth techniques for the fabrication of nanoobjects. More specifically, I worked in the MAT2D group that is specialized in the fabrication of 2D materials and stackings of 2D materials (Van der Waals heterostructures). The team is also expert in characterization of 2D materials. They study the optomechanical properties of suspended 2D material and of electrical and structural properties by ARPES (Angle resolved photo emission spectroscopy), AFM (atomic force microscopy) and various others measurements. The team is composed of 8 peoples (4 permanents and 4 non-permanents). My internship supervisor is Julien Chaste, specialized among others in opto-mechanical properties in 2D materials and in stackings of 2D materials.

3 Presentation of the internship subject

3.1 State of the art

Thermal conductivity is a physical quantity that is of great interest in our life. In the 3D search field, some materials were found with high or low thermal conductivity and high electrical conductivity [17]. Depending of the size of the sample and the temperature, we can have different regimes of heat transport through phonons [2]. At extremely low temperature, we access to the ballistic regime. In this case, all phonons scatterings come from the dimensions of the materials. The heat carriers propagate without scattering through the whole system. Figure 1 shows the regimes as function of the temperature for a nanostructure and a 3D material. In 3D material, at high temperature, the diffusive regime reigns on the propagation. Indeed, the main regime in 3D material is the diffusive one. This regime includes some scatterings that diffuse the heat and produce energy dissipation. This regime is due to the 3-phonons Umklapp scattering that is dominant in 3D material. This Umklapp-process does not hold the total momentum of the phonons. As a consequence, there are heat dissipation. The heat transport follows the Fourier's law ($q = -k\Delta T$ with q heat flux density, k thermal conductivity and ΔT the temperature gradient). The behavior of heat diffusion in 3D material is well known in this case. However, Umklapp-processes are not the only processes that contribute to scattering. A second 3-phonons process – Normal process – contributes to scattering. This process holds the total momentum of the phonons constant. It does not dissipate the heat as the Umklapp-processes. In 2D materials and nanostructures, the Umklapp contribution to scattering is negligible. Normal processes dominate. That decreases the heat dissipation as we know it. It does not follow the Fourier's law anymore [11]. A new regime appears at this point. The heat transport is neither ballistic nor diffusive. It follows a regime similar to Poiseuille regime for liquids [2]. On the figure 1, this regime appears to dominate the thermal propagation on a higher range for nanomaterials than for bulk.

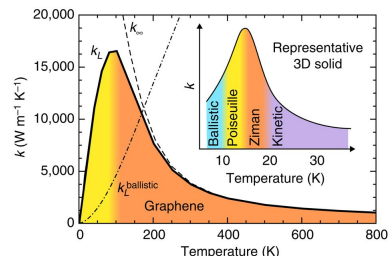


Figure 1: Thermal conductivity regimes of graphene ribbon. Inset: thermal conductivity regimes in a 3D material. From [2].

The phonons do not only contribute individually to the heat transport. Collective phonon excitations are also heat carriers. Moreover, a wave phenomenon appears similar to the sound. That is the second sound propagation. It was shown in graphene [6]. All these behaviors decrease the pertinence of the usual modellings. Preliminary theoretical works were done showing this behavior [2, 11]. Some experimental ones were done in Graphene [6]. For other 2D materials, there are still experiments to do to confirm or not this regime of heat transport. Moreover, better models including 2D materials are of interest.

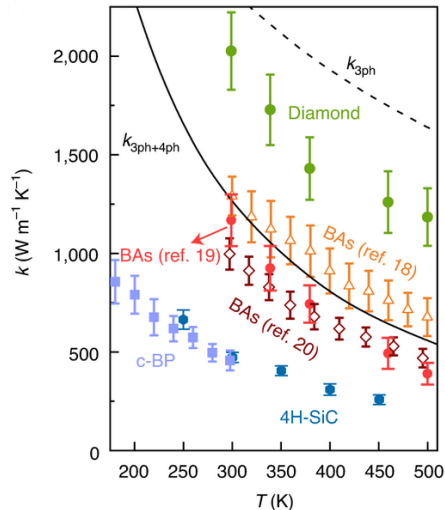


Figure 2: Temperature dependant thermal conductivity of few 3D material. From [17].

gives rise to anisotropic physical quantities. For example, the thermal conductivity is much lower in the out of plane direction than in-plane one. It opens a full playground for new experiments. Thermoelectric quantities such as Seebeck coefficient (coefficient measuring the conversion of temperature gradient to electrical difference of potential) and the zT figure of merit are quantities that can be high in 2D materials. These quantities are of great interest in we want applications for our material. Indeed, Seebeck coefficient is the one that is responsible of the conversion of electrical energy in thermal one and vice versa. If we have important coefficients for them, we can have applications in energy conversion.

3.2 Scientific problems to solve

To realize the experiments in order to understand the heat transport, some techniques are already known to heat the sample. As in 3D materials, 2D materials can be heated by Joule effect [4]. To be able to understand how the heat propagates, we must avoid dissipation along other canals of heat dissipation. For this purpose, an insulating layer as ground layer is often used. Another technique that is on progress is to suspend 2D materials [14]. That avoids all substrate dissipation if we put the sample under vacuum. This technique is not fully easy to achieve. To realize this suspension, we need to transfer the 2D material on our structure. This is already mastered [8] and a lot of improvements were done from the beginning of the transfer issue [13, 22]. It is still difficult to implement it experimentally.

An important characteristic of the 2D materials is their great variety. There are semi-conductors, metals and insulators. There are monoatomic, alloys. This diversity allows to have a wide spectrum of properties. The thermal conductivity can reach with graphene $4000 \text{ W.K}^{-1}.\text{m}^{-1}$. It can also decrease to $0.64 \text{ W.m}^{-1}.\text{K}^{-1}$ with InP_3 [18]. The available spectrum reaches the extreme values we can have with 3D materials. Indeed, the temperature dependant thermal conductivity of the extremum 3D materials is visible on figure 2. The maximum thermal conductivity is for diamond at $2000 \text{ W.m}^{-1}.\text{K}^{-1}$ [17]. That is lower than graphene. For low thermal conductivity, 3D materials are also overpassed by nanostructures. It is possible to obtain low thermal conductivity in 3D materials but at the cost of high anharmonicity and heavy material [17]. For 2D material, the limit of low thermal conductivity can decrease even more with heterostructures. These structures are composed of layers of different 2D materials. The combination of different materials gives rise to new properties over-passing the 3D materials [21]. That comes from the fact that the interactions between the layers is very different from bulk material.

Another specificity of 2D materials is their anisotropy. 2D materials is one layer of a material. Most of the time, the interest is in these monolayers. The interaction that we have between the layer and the substrate is different from the ones we have inside the layer. That

3.3 Specificity of the subject

Our problem is to determine the thermal conductivity in 2D materials and to understand how this one changes. Under this problem, multiple problems are hidden. We need to determine if the Joule effect is big enough and we need to have resolution of our tool that measures temperature variations good enough to see the variation of the heat. The spacial and temporal resolution must also be good enough to measure the variations. If we have good enough resolution, it is possible to measure the thermal conductivity. The tool that we use for that is a micro-Raman spectroscopy. This spectroscopy is a non-invasive technique that allows to understand our device without destroying it. Moreover, the spatial resolution of the Raman spectroscopy can be of 0.5 micrometer. This technique is promising to have precise and in-situ measurements.

2D materials are non-common materials that are very sensitive to the external medium. In our case, we don't work with millimeters continuous layers of 2D material with area of few millimeters square. We work with flakes with an area of hundreds of microns square. If we work with suspended materials, we could obtain different morphologies for our sample that would allow better comprehension of our material.

3.4 Objectives

The goal of this internship is to measure thermal conductivity of 2D materials. At this purpose, we need to see the behavior of the Raman spectrum of the 2D material as function of the temperature. That allows us to calibrate our sample. We can also see how the Raman spectrum changes as a function of other parameters (stress, concentration in components) in order to uncorrelate the change of the Raman spectrum due to the temperature to the other parameters. Another important goal is to transfer the 2D material on the wanted substrate. We want to transfer the 2D material such that this one is suspended between 2 heaters. With this setup, we would be able to see the change of temperature without dissipation in others mediums if we do it under vacuum. At last, the main objective is to heat our sample and to observe the behavior that our sample exhibits.

4 Results

The first part of this internship consists in the characterization of the 2D materials I wanted to study. The materials that are of interest are 2D materials such as InTe, $WS_{2x}Se_{2(1-x)}$, MoS_2 , WSe_2 and h-BN. The materials that we use come from different places and are elaborated in different ways. For InTe, WSe_2 and h-BN, the materials were exfoliated from a crystal using tape and repetitive tape transfer till the material become thin enough to be considered to be a 2D material (few nanometers thick). $WS_{2x}Se_{2(1-x)}$ and MoS_2 were grown by CVD. $WS_{2x}Se_{2(1-x)}$, MoS_2 and WSe_2 are transition metal dichalcogenides and semiconductors. h-BN is an electrical insulator.

4.1 Setup

To characterize the 2D materials as function of the temperature, we need a tool to change the temperature and a tool to measure it. The tool that we use in order to calibrate the change in temperature is a Linkam cell. This cell is attached to a liquid nitrogen reservoir that allows to decrease the temperature of our sample. It also contains a resistance that can heat up the sample. Combining both systems, it is possible to reach temperature from $-192^{\circ}C$ to $600^{\circ}C$. This cell is put under vacuum such that no water condensation should appear in the cell. The vacuum setup is also important to hold the material stable since it can react with the outside particles or oxygen otherwise. That also avoid dissipation through the air that could modify the temperature of the material.

In order to see the change of temperature of our material, we use confocal Raman spectroscopy. This spectroscopy is a non-invasive way to observe our sample without destroying or changing it. It consists of sending a laser beam at a certain wavelength and, by analyzing the reflected light, it is possible to have access

to the phonons of the sample. The light of the laser is filtered by a notch filter and we only detect the light at different energy from the one of the laser (in our case lower i.e corresponds to Stokes processes). The energy of the laser is transmitted to the sample. It is possible that an interaction between the photon and a phonon appears. Both energies may be added to bring an electron to a higher energy. The electron may turn back to its original level with a radiative relaxation. In this case, the energy that the electron releases will be higher than the one of the laser. This mechanism is the Anti-Stokes scattering as on the figure 3. The energy that the laser gives to the sample can also bring directly to a high energy electron level. The relaxation may be decomposed in 2 mechanisms. Part of the energy may be used to bring the electron to a lower energy level by a radiative relaxation. Another part of the energy may be dissipated by formation of a phonon. That is the Stokes mechanism as on the figure 3. When we look at the radiative emissions, we can deduce which phonons appear from this interaction. Since the phonons energies are quantified, only some energies are available. Each phonon resonance corresponds to a vibration in the sample. Raman spectroscopy is only sensitive to vibration with even symmetry and detect them.

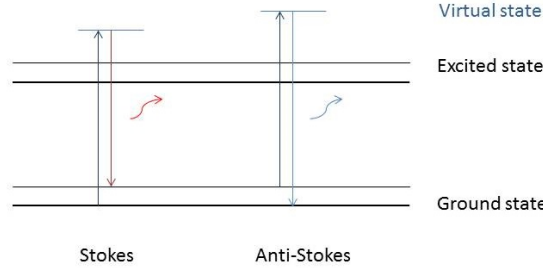


Figure 3: Scheme of the different radiative processes.

For our Raman spectroscope, the reemission that we observe is at lower energy than the one of the laser.. The energies of the available phonons change as function of the temperature. When the temperature changes, Raman peaks may shift. For each crystalline structure, the phonons are different. It is possible to recognize the materials by looking at their Raman spectrum. The Raman spectrum does not give us only information about the vibrations themselves and the temperature. The phonon energy also differs as function of others parameters such that the stress in the structure, the concentration of the different components of the material. That is important to be able to uncorrelate the different origins of the Raman spectrum shifts. At this purpose, we can use the Photoluminescence spectrum. Using a laser beam as previously, we excite the sample. But we don't look at the energies very close to the laser one. That means that the intraband relaxations till the bandgap are not of interest. We are interested in the vertical interband transitions . In case of a semi-conductor, if the gap is direct, we have an important peak corresponding to the recombination of the exciton. The reemission corresponds to the radiative relaxation of the electron from the conduction band to the valence band. If the gap is indirect, the peak is less important and wider. As for the Raman spectrum, the Photoluminescence spectrum depends on the structure of the material. Combining both methods allows us to get more information on our material and to access to the origin of the shift. Raman spectroscopy is a very interesting tool since the measurements that we do with it are only localized in the illuminated-by-the-laser-beam part of the sample. That allows us to map our sample and to have a resolution of $0.5 \mu\text{m}$ on our material. It is possible to observe a gradient of temperature inside our sample. That can be useful to see the heat propagation in our setup.

4.2 Use of Raman spectroscopy for sample characterisation

In this part, we introduce our methodology for the optical separation for the different 2D materials properties. The first thing we wanted to do was to observe a single flake without temperature variation. The sample that we observed was $WS_{2x}Se_{2(1-x)}$ (a ternary material). Since this material was grown by CVD, the concentration of Se and S can be different depending on the localization on the flake. For this sample, the interesting thing was to track the concentration of S and Se depending on the position on the WSSe flake. To determine it, we can realize Raman spectra everywhere on the sample. The peaks that we observe are corresponding to the different available optical phonons in the sample. The ones coming from interactions between W and Se decrease in intensity when the concentration in Se decreases [5]. Using a calibration, it is possible to turn back to the concentration by comparing the peaks intensities.

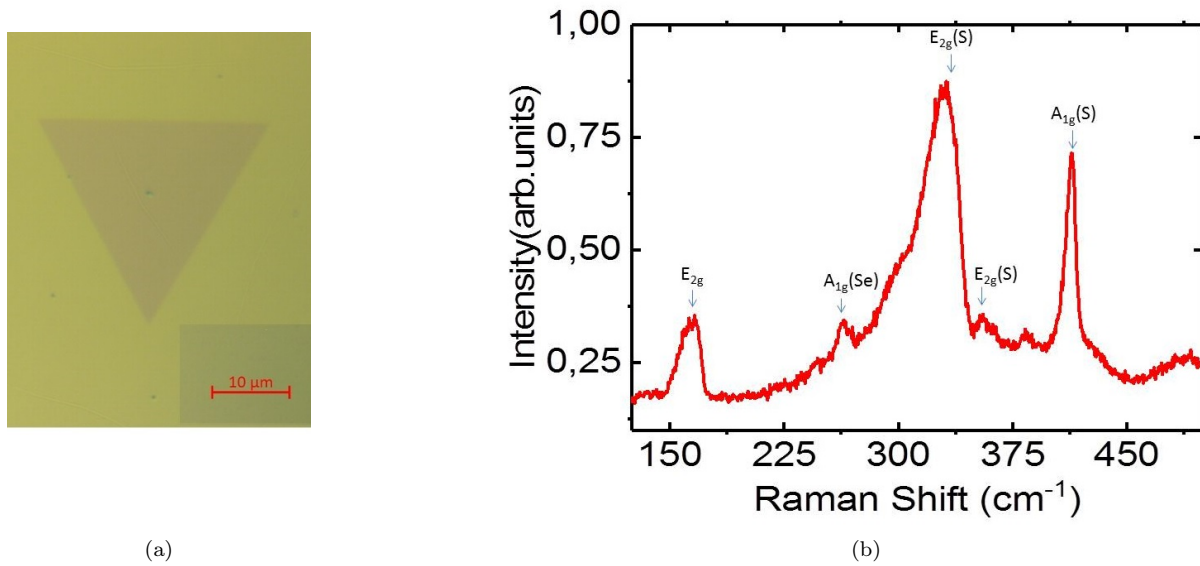


Figure 4: Preliminary observations on the $WS_{2x}Se_{2(1-x)}$ flake (a) Optical image of the $WS_{2x}Se_{2(1-x)}$ flake. (b) Typical Raman spectrum done with a laser at 532 nm on $WS_{2x}Se_{2(1-x)}$ flake with its characteristics Raman peaks.

Figure 4 (b) represents the Raman spectrum on a spot of the $WS_{2x}Se_{2(1-x)}$ flake that can be seen in the optical microscopy image in figure 4 (a). It is composed of different peaks that we can attribute to specific vibrations. The peaks at 162, 329 and 358 cm^{-1} are E_{2g} peaks attributed to the interaction between W and S. The peak at 265 cm^{-1} is a A_{1g} peak attributed to the interaction between Se and W. The peak at 413 cm^{-1} is a A_{1g} peak attributed to the interaction between S and W. This Raman spectrum is typical of $WS_{2x}Se_{2(1-x)}$ [5]. The Raman spectrum is similar from one spot to another on the flake but the peaks vary in intensity and position depending on the variations of concentration and stress. We scan the flake by looking at the spectrum at each point. We focus our attention on a specific peak. With a Raman scan, we check how the intensity of a peak varies. We also establish if there is a shift in the peak's position.

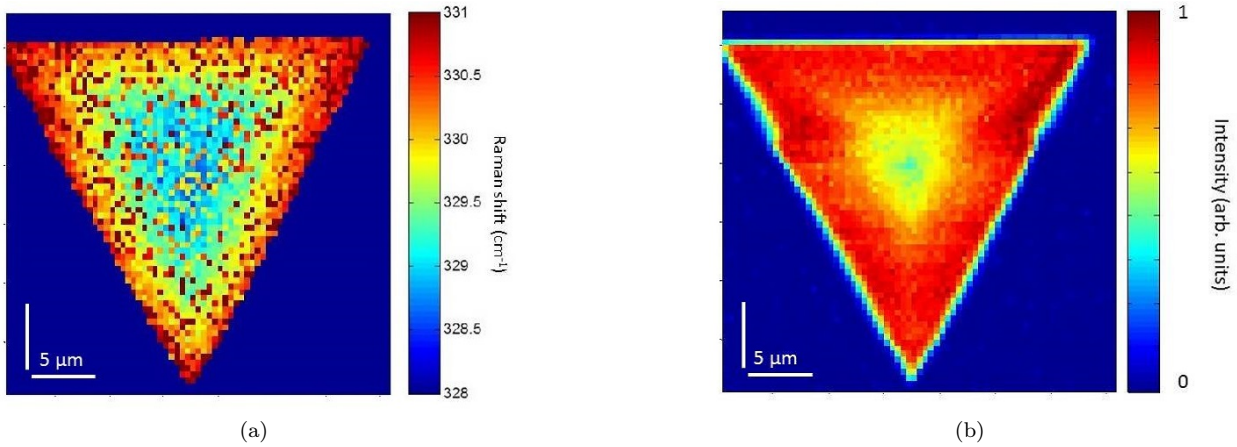


Figure 5: Maps from the Raman spectrum scan with a laser at 532 nm (a) Position of the Raman peak around 329 cm^{-1} corresponding to a E_{2g} (W,S) peak . (b) Intensity map of the Raman peak around 329 cm^{-1} corresponding to a E_{2g} (W,S) peak of a $WS_{2x}Se_{2(1-x)}$ flake.

The map 5 (a) shows the position of the maximum of the Raman peak around the value of Raman shift equal to 329 cm^{-1} . This peak corresponds to a E_{2g} (W,S) peak. As we can see, the Raman shift is globally higher on the edge of the flake (331 cm^{-1}) and it is lower in the middle of the flake (329 cm^{-1}). There are multiple parameters that can influence the Raman shift. The concentration in S is one of the parameter. However, stress is also another one. It is possible that there are some strains in the structure and some concentration variations. To determine which parameter is responsible for this shift, we need another map that is dependant of less parameters. The figure 5 (b) shows the different intensities that we have for the same peak (329 cm^{-1}). For this peak, the intensity exhibited by the flake is lower in the middle of the flake than on the edges. Concerning the intensities of the peaks, we consider that the main parameter that changes them is the concentration. The intensity's variation is much higher than the position's variation of the shift when varying the concentration ([5]). With this map, we can examine how the concentration of S and Se vary in the sample.

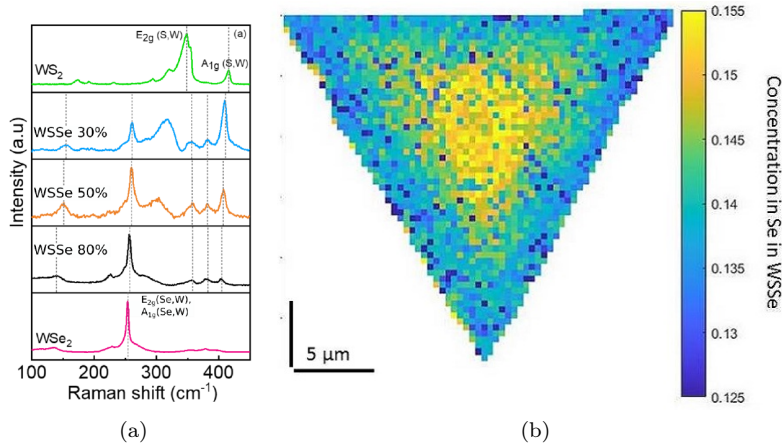


Figure 6: Determination of the concentration in Se (a) Raman spectra at different concentrations of Se in WSSe. From [5] (b) Map of the proportion of Se in a $WS_{2x}Se_{2(1-x)}$ flake.

On the spectra 6 (a), when the concentration in Se increase, the peaks associated to Se increase in intensity and the ones associated to S decrease in intensity. By calibration we determine the concentration of Se everywhere on the flake 6 (b).

On the map 6 (b), we see that the concentration of Se in $WS_{2x}Se_{2(1-x)}$ varies between 13.25 % on the edges and 15.60 % in the middle. The Se concentration is the most important in the center of the flake. This concentration variation comes from the synthesis of $WS_{2x}Se_{2(1-x)}$. The variation in concentration of Se is diffusive with a low fluctuation.

To realize this concentration map, we only took the intensity of the peaks into account. We let on the side the Raman shift position. If there is a variation of 2.4% of the concentration, the Raman position shifts of 0.047 cm^{-1} . This is not visible on the Raman spectrum that we have and can be neglected. Nonetheless, shift on the positions of the Raman peaks appear. The shifts that we observe on the map 5 (a) come from others physical quantities than the concentration.

Stress is one of the quantities that acts on the Raman peak's position. Indeed, stress influences the distance between the atoms and the energy of the corresponding vibrations changes. That induces a shift of the Raman peaks. This shift is larger for $E_{2g}(S,W)$ peaks than for $A_{1g}(S,W)$ peaks [3]. The observation of a higher shift for $E_{2g}(S,W)$ peaks than for $A_{1g}(S,W)$ peaks is a strain signature.

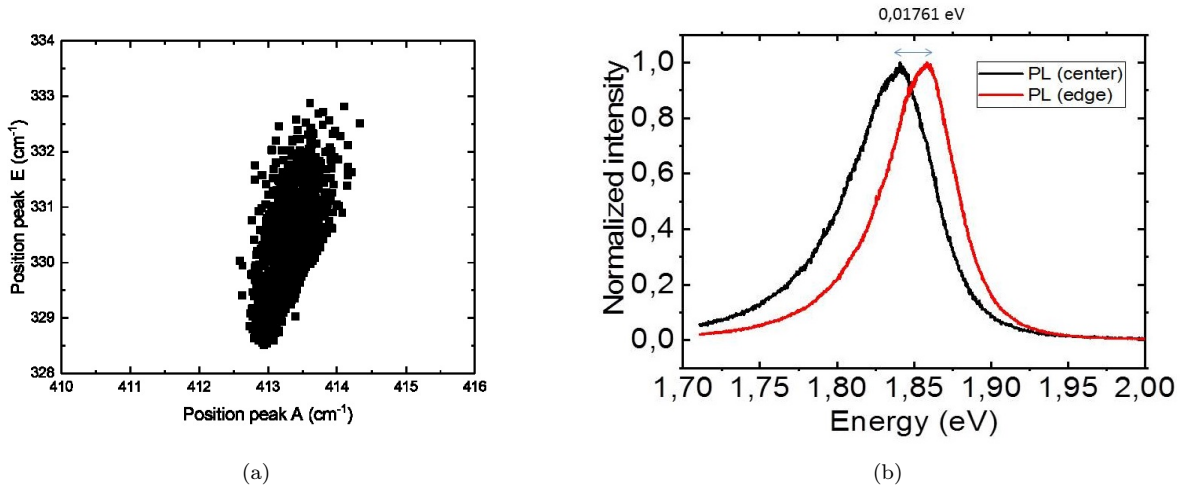


Figure 7: Strain signature (a) Diagram of the peak $E_{2g}(S,W)$ at 329 cm^{-1} as function of the peak $A_{1g}(S,W)$ at 413 cm^{-1} showing a higher dispersion of $E_{2g}(S,W)$ as of $A_{1g}(S,W)$ (b) Photoluminescence of $WS_{2x}Se_{2(1-x)}$ at the center and the edge of the flake with a laser at 532 nm. There is a variation of 17.61 meV between the maximum of both spectra.

We plot in figure 7 (a) the position of the peak $E_{2g}(S,W)$ at 329 cm^{-1} as function of the peak $A_{1g}(S,W)$ at 413 cm^{-1} in order to determine if stress is indeed the parameter that alternate the spectrum. This diagram is composed of all the Raman spectra taken on the flake. Each of them corresponds to specific parameters of the sample (concentrations, strain). The main parameter that change the $E_{2g}(A_{1g})$ graph can be find from the slope that this diagram seems to show. If the slope is equal to one, the shift is due to temperature difference. If it is superior to one, the shift comes from the stress. If it is inferior to one, the shift comes from the doping [10]. As we can see, the position of the $A_{1g}(S,W)$ peak shifts of 1 cm^{-1} whereas the position of the $E_{2g}(S,W)$ peak varies of 4 cm^{-1} . That confirms that there are strain in the structure [10]. In this sample, the stress deviation is a bit less than 1%.

It is not the only way to see that there is a strain in the structure. The Photoluminescence (PL) spectrum also emphasizes the strain signature. On the figure 7 (b), we have PL spectra of the flake that we took both

near to the middle of the flake and near to the edge of this one. We see that there is a shift of 17.61 meV between both spectra. Both of them have the same shape. Depending of the strain, the band structure changes. That changes the gap between the conductive levels and the insulating ones [1]. The PL changes because of that.

The combination of the PL and the Raman spectra should allow to access to more data on the material that we have. Nonetheless, the reunion of both information didn't work as expected. We had a mismatch between the value of the stress that we obtain with the Raman and with the PL. Nevertheless, PL and Raman are interesting tools to determine the characteristics of our material. We can use them to determine the stress, the concentration. We can also use them to determine the temperature and that will be our purpose.

In this part, we observed a flake that was put on a SiO₂ wafer. It is also possible to observe other configurations of 2D materials. Moreover, we can observe them while we apply a constraint on the material.

4.3 Electrical heating by Joule effect of 2D material on substrate

An important part of this subject is the ability to heat up a sample. An interesting lead that we can follow to heat a sample is to use the Joule effect.

The first that we are looking at is a circuit where the 2D material of interest is put on a sample and is part of the electrical circuit. This sample was provided by Maria-Luisa Della Rocca and Salvatore Timpa from the MPQ laboratory. We can apply a voltage (V_{DS}) on the material and observe the current that passes through the 2D material. By this means, we obtain the I(V) curve that gives us the impedance of the sample and allows us to determine the behavior of the device. The gate is done in gold and separated from the flakes with h-BN flakes.

On the optical microscopy image 8 (a), we see the samples that we study. There are two similar devices. The device SO4 on the top of the image and the device SO2 on the bottom of the image. Both devices are constituted of two gold gate contacts (not visible on the images) that are connected to the gate. On this gate, between 30 and 40 nm of h-BN are deposited in order to isolate the WSe₂ from the gate. On top of it, few layers of WSe₂ are deposited. For the device SO4, there are between 2 and 3 layers whereas for the device SO2, 4 layers are deposited. A source and a drain gold contacts are present to apply V_{DS} to the material. With these devices, it is possible to apply V_{DS} and V_G .

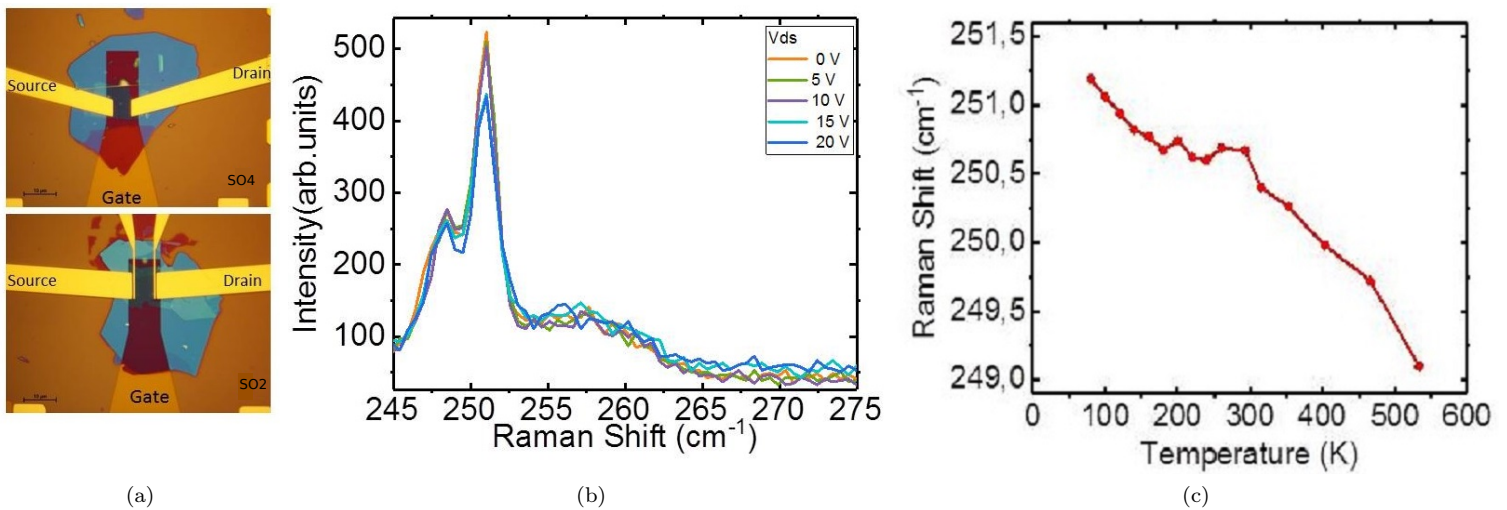


Figure 8: Raman and optical microscopy image of the sample (a) Devices with WSe₂ on h-BN (b) Raman spectrum of the device SO4 at different V_{DS} with V_G equal to 50 V (c) Temperature calibration of the Raman peak E_{2g} (W,Se) around 250 cm^{-1} .

On the figure 8 (b), there are the Raman spectra taken at 5 different V_{DS} between 0 and 20 V when a gate voltage of 50 V is applied on the sample. The spectra are composed of a $E_{2g}(W,Se)$ peak at 251 cm^{-1} . On the figure, we see that when we vary the voltage V_{DS} , there are no change on the Raman spectrum. The peak remains at the same Raman shift. On the figure 8 (c), we can see a calibration of the same Raman peak $E_{2g}(W,Se)$ position when we change the temperature. This calibration was done using the Linkam cell to change the temperature. The measurements were done between -192°C and 260°C . The peak shifts by 2.09 cm^{-1} for a temperature difference of 453 K. It is $0,0046\text{ cm}^{-1}\cdot\text{K}^{-1}$ so the sensitivity is around tens of K. We have a decrease of the Raman shift position and it is coherent with other experimental works [12].

Since no shift is visible on the figure 8 (b), no heating appeared. That means that even when we apply a voltage $V_{DS} = 20\text{ V}$ with $V_G = 50\text{ V}$, it is not enough to heat up the sample by Joule effect because the sensitivity is high enough to see the heating if this one is over 20°C .

To better understand our sample, we also realized $I(V)$ curve to see the behavior of our device.

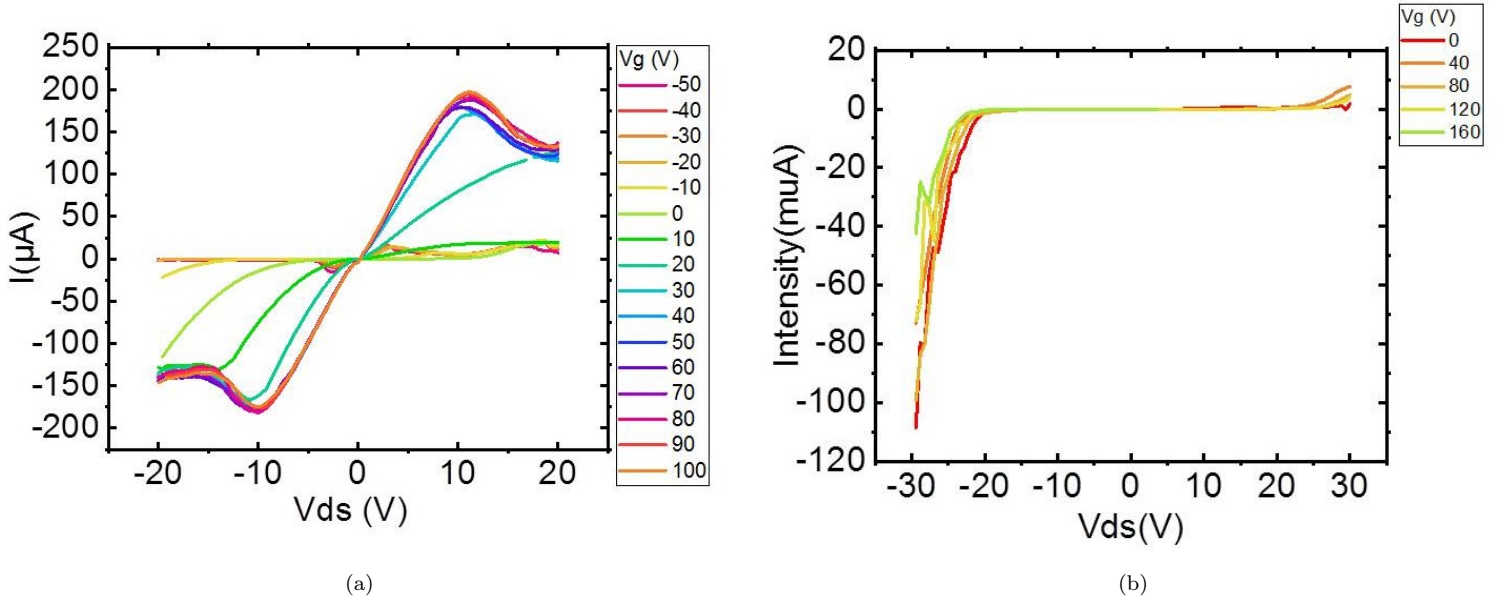


Figure 9: $I(V)$ curves of both devices (a) $I(v)$ curve of the device SO4 showing a negative differential conductance at V_g superior to 50 V. (b) $I(V)$ curve of the device SO2 showing a behavior similar to the one of a diode.

The $I(V)$ curve 9 (a) corresponds to the device SO4 on which we measured the Raman spectrum. When a gate voltage superior to 50 V is applied, the current is linear with V_{DS} from -10 to 10 V. The maximum intensity achieved is at $200\text{ }\mu\text{A}$ when V_{DS} equal 10 V. Then the intensity decreases to $150\text{ }\mu\text{A}$ when V_{DS} increases to 18 V corresponding to a power of 3 mW. The intensity remains then constant until $V_{DS} = 20\text{ V}$. In the negative voltages, we also have more or less the same behavior. We have negative differential conductance. It was already observed in MoS_2 [4]. In this article, it was attributed to the self heating and the scattering of electrons by hot optical phonons. That is not coherent with the observation that we have in our case where we show that there are no heating. But it may be due to the presence of h-BN which tend to cool down the electrons [23, 19, 16]. Indeed, in heterostructure of graphene and h-BN, a out-of-plane energy transfer channel can exist between both materials [19]. That transfers the heat in the h-BN due to its hyperbolic electronical nature of this material. A saturation of the current was observed in the case of graphene. Even if in our case, we have a semiconductor, the observed behavior may be linked to the same phenomenon.

When a gate voltage inferior to 50 V is applied, the behavior with the negative differential conductance is less visible. The intensity drops of 2 magnitude. At V_g equal to 0, the behavior seems more like a diode one. When we put V_{DS} inferior to 0 V, another negative conductance appears but this time at a lower intensity ($\approx 15\mu A$) when a potential V_{DS} of 2.6 V is applied.

For the device SO2, the I(V) curve 9 (b) shows the behavior of a diode. The current is nearly equal to zero for V_{DS} from -20 to 20 V. It increases then quasi linearly until the maximum value is reached. That comes from a Schottky barrier that may appear between the metallic contact and the semiconductor material. It was impossible to overcome this Schottky barrier. Without V_G , it was possible to achieve an intensity of $-110\mu A$ when -30 V is applied as V_{DS} . That was the maximum value that was achievable. We see that for both samples, we did not achieve the heating of the sample. One of the reasons of it can be the fact that the material is not suspended. H-BN, even if has a low thermal conductivity in the out-of-plane direction, can have a high conductance. At the end, there are dissipation through the substrate and there will be no heating.

We could ask us if with suspended materials, we can have better heating.

4.4 Electrical heating by Joule effect on suspended 2D materials

For this purpose, the team (and more Anis Chiout - PhD in the team) tried to heat up another 2D material (MoS_2) with similar characteristics (semiconductor). Its material was monolayer and suspended over a hole.

The setup was as shown on the scheme 10 (a) . The 2D material was suspended on a membrane of $3,5\mu m$ and a V_G and a V_{DS} was applied on the membrane through gold contacts. As wanted for the sample on h-BN studied previously, the difference of potential induced an heating by Joule effect. The optical microscopy image 10 (b) is one of the typical membranes that was studied. The darker color of the hole than the neighboring holes is characteristic of the presence of the membrane. On the image, the dotted-red lines are the boundaries of the deposited flake of MoS_2 . On the figure 10 (c), we can see the Raman spectrum of MoS_2 without excitation with its characteristics peaks E_{2g} and A_{1g} respectively at 384 cm^{-1} and 407 cm^{-1} . It is the reference for the Raman spectra without heating of the sample.

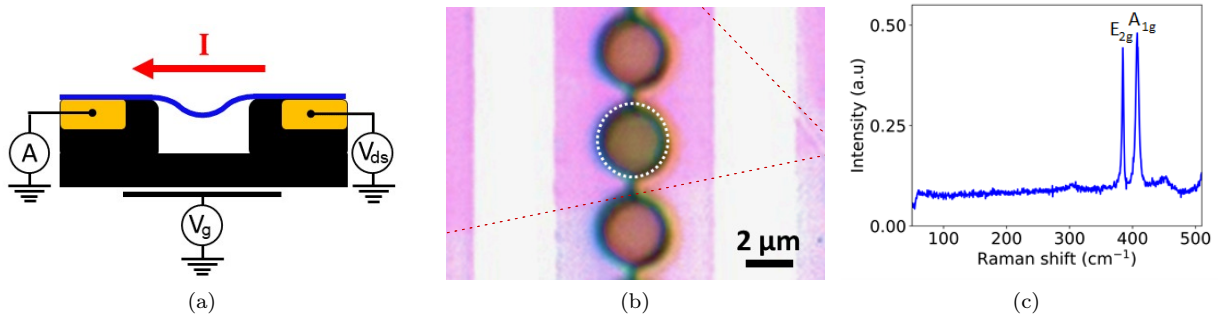


Figure 10: Setup (a) Scheme of the transistor configuration, MoS_2 (in blue) is suspended between two gold electrodes allowing to apply V_{DS} and measure the current which allows to heat the membrane. Si substrate is used as back gate for both DC and AC excitations. (b) Optical microscopy image of a typical sample. MoS_2 drum (dotted white circle) is between two electrodes (c) Raman Spectrum of MoS_2 measured with a laser at 532 nm with its characteristics peaks.

Once we know the characteristics of the sample that we want to heat, we can apply a voltage and see the reaction on the current. In this sample, we extracted the power that was applied on it. To do it, the formula $P = IV_{DS}$ was used.

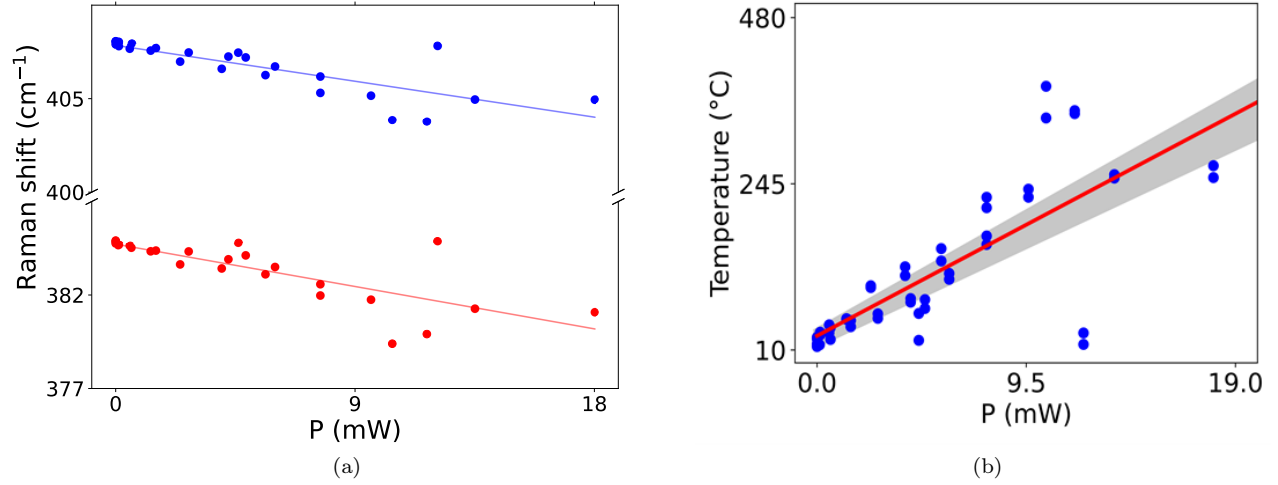


Figure 11: Behavior when power on (a) Variation of the A_{1g} (blue) and E_{2g} (red) with respect to the heating power. The peaks are shifting while we increase power linearly (b) Temperature of the membrane extracted from the Raman peaks shift, there is a linear dependence between the temperature and the heating power.

On the figure 11 (a), we see the variation of the A_{1g} (blue) and E_{2g} (red) position peaks when a voltage V_{DS} is applied on the sample. Both of them decrease when the applied power increase. Since the Raman shift decreases with the temperature, this shift proves that there is a heating of the material. It is even more visible on the figure 11 (b) that shows directly the temperature shift as function of the applied power. On this graph, we see that the temperature reached by Joule effect overpasses 250°C when the applied power is superior to 10 mW. From the paper [9], we extract the Raman shift as function of the temperature. The A_{1g} and E_{2g} shifts decrease by $1,6 \text{ cm}^{-1}/100\text{K}$ and $1,3 \text{ cm}^{-1}/100\text{K}$ respectively for a monolayer and $1,3 \text{ cm}^{-1}/100\text{K}$ and $1,5 \text{ cm}^{-1}/100\text{K}$ for a multilayer. The rise of the temperature is linear with the applied power. The increase in temperature is well linked to the voltage that we apply. If we compare this device with the non-suspended 2D material studied previously, we see that there is a huge difference in the 2D material behavior. The maximum power that was accessible with the non-suspended material was $P = IV = 150 \cdot 10^{-6} \cdot 20 = 3 \text{ mW}$. For this power, we already had Joule heating with the suspended device. With the non-suspended, we do not. That tends to prove that it is of great interest to suspend the material we want to study. Moreover, suspended membranes can also be of interest to study the optomechanical properties of the samples. Since there are membranes, they can vibrate at different frequencies. These resonance frequencies will change with the temperature at which we are. If we look at the shift of the frequency, it is another way to turn back to the temperature of the membrane than by looking at the Raman spectrum.

It would be interesting to test this hole configuration for other 2D materials. For this purpose, we need to transfer 2D material on holes. To change the shape on which we deposit the 2D material can also allow us more freedom. For all these configurations, there is a step that we can't avoid. This is the transfer. It was done on the sample Anis Chiout studied and have to be repeated with other materials to characterize them.

4.5 Technique of transfer on holes

I have participated on the transfer of these suspended MoS₂ samples by doing my own transfer. The main steps consists on the decoupling of the 2D material from the substrate. Then, we chose a flake and transfer it on the wanted sample. A last step of cleaning is required when the flake is not fully clean because of the transfer manipulation.

For CVD grown 2D material such as MoS₂ and WSSe in our case, the interaction between the 2D material and the substrate is quite important. Because of that, we first need to transfer all our flakes on a new planar substrate before trying to take the wanted flake. To remove the 2D materials from the substrate, we need to provide them a substrate that has a stronger surface interaction with our 2D material than Si (or SiO₂). That is why we use Polymethyl methacrylate (PMMA) to remove the 2D material. This polymer acts as a tape on which the 2D material hangs on. The process that we follow is the one below (figure 12).

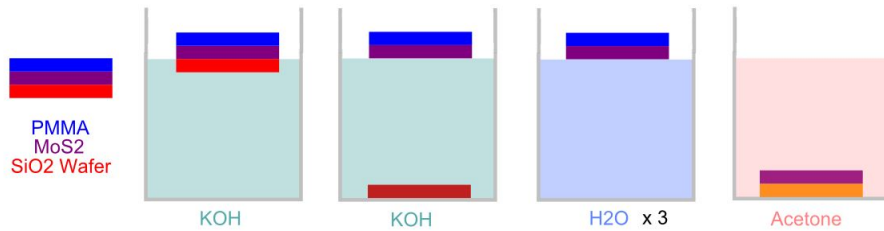


Figure 12: schema of a wet transfer procedure.

This procedure is called a wet transfer procedure. We first spincoat a layer of PMMA on the 2D material that we want to take. Then, we put the sample in a solution of KOH that remove the bonds between SiO₂ and PMMA by damaging PMMA. The 2D material remains on PMMA and is decoupled from the Si substrate. The Si substrate sinks to the bottom of the solution and the PMMA -on which the 2D material remains - remains at the surface of the liquid. It is possible to fish the PMMA with a bowl at this moment. After 3 dip rinsing with water, it is then possible to fish the PMMA with another substrate (bright yellow on the scheme) on which the 2D material remains weakly coupled. We let it dry and we put it in acetone during a night. The PMMA dissolves in acetone. After washing it a last time with isopropanol, we obtain our 2D material on the substrate we chose without PMMA and with weaker bonds between the substrate and the 2D material. Once we have this transferred 2D material, it will be easier to take a single flake from the sample. Moreover, this technique can also be used if we just want to change the substrate of the 2D material.

If we want to put our sample on a hole, the previous technique is not a good one. It is not precise enough and the immersion in acetone may destroy the structure. To solve these problems, we use a dry transfer. Without putting in a liquid, we try to take away the flake that we want from the substrate. A transfer station is a tool that helps us to have a precise and controlled pick-up of the flakes. It is constituted of a microscope and two sample holders on the horizontal plane that we can approach the one from the other as shown figure 13 (b). The ground sample holder is connected to a heater. We approach both sample holders slowly such that the contact between both samples are very small (diameter of about 0.5 mm is reachable). We can not directly put in contact the two plane samples. We use an intermediate that is responsible of the pick-up and the release of the flake. This intermediate is a bubble of Polydimethylsiloxane (PDMS) on which we deposited PMMA by spincoating. Then we can proceed to the transfer.

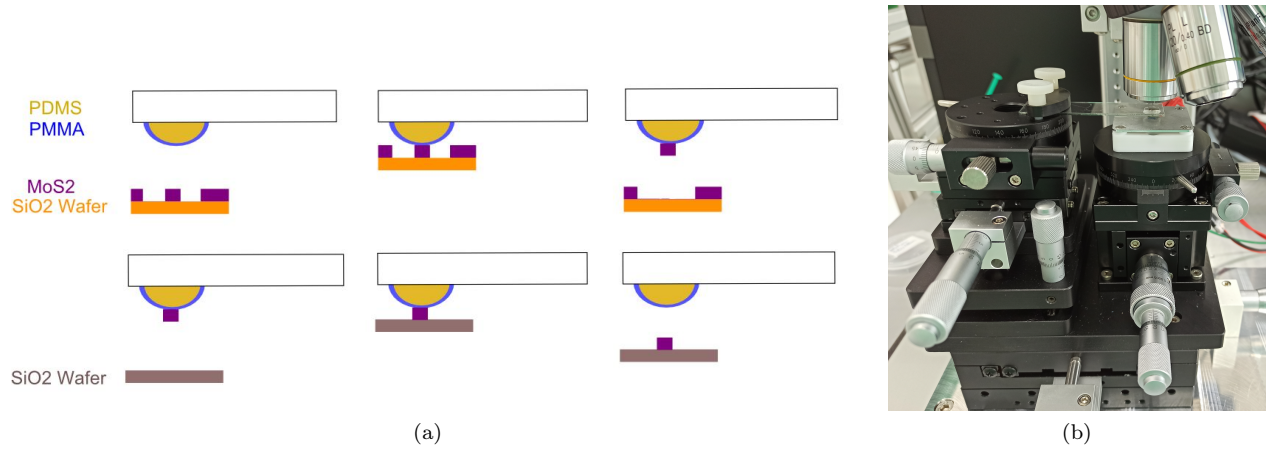


Figure 13: scheme of a dry transfer and photography of the transfer station.

The procedure we developed is the following one shown on the scheme 13 (a). Basically, the first three steps consist to catch the flake that we want. The three last are the one to release the flake on the surface. The figure 14 shows us different steps of the dry transfer. We approach the bubble from the 2D material until it touches, we increase the temperature of the sample with the 2D material to 60°C. This step allows to relax the PMMA all around the flakes. That increases the contact area with it. It is the step showed on figure 14 (a). It is important to choose the contact area to catch the flake we want as the three on this picture. After this heating step, we turn back to an ambient temperature. Then, we add a droplet of water near to the contact area. By capillarity, this droplet moves away the PMMA from the substrate. When we expelled the PMMA from the Si substrate, it takes with it the 2D materials flakes. We move slowly the bubble of PDMS away from the Si substrate on which was the 2D material. The 2D material comes on the bubble. Once we have the 2D material on the bubble, we need to deposit it on the sample that we want. Using the same setup, we approach the bubble to the new substrate. We make them touch each other. We increase the temperature to 180°C to deposit the PMMA and the 2D material on the sample. This step is shown on the figure 14 (b) where we see the circle corresponding of the contact area between the substrate with holes and the PMMA on which are the flakes. After this step, the PDMS bubble is taken away from the substrate. The flakes are deposited on the holes but PMMA also covers all the surface.

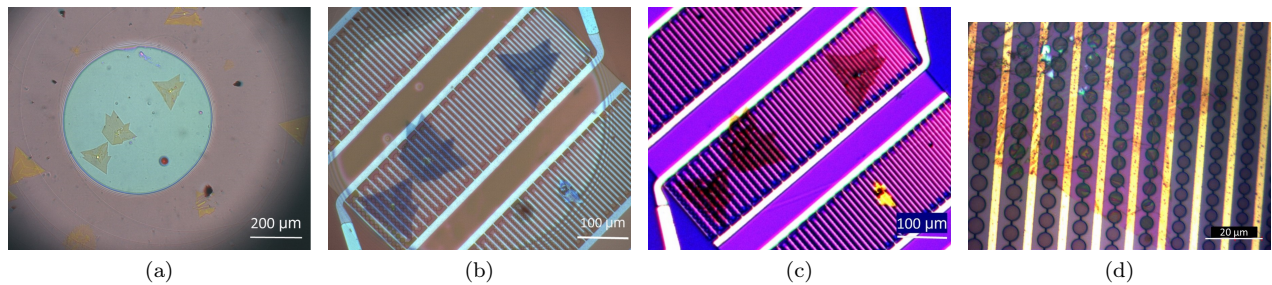


Figure 14: Optical microscopy images of different steps in the deposition of WSe2 on holes (a) Flakes on the substrate and contact with the PMMA. (b) Flakes on PMMA taken from the substrate. (c)-(d) Flakes on the final substrate after dissolution of PMMA in acetone and use of a critical superdryer.

The PMMA needs to be removed from the 2D material to obtain clean samples. For that, we can use an oven in vacuum. Putting it few hours in an oven at 350°C allows a slow evaporation of PMMA. This

velocity provides a homogeneous evaporation such that the 2D material is not stressed by this removal and remains on the holes. Another solution that we used is to use a critical superdryer to avoid capillarity tension when we put the sample out of the solution of acetone that decompose PMMA. For this method, we first put the sample in hot isopropanol at 70°C. This solvent has a very low capillarity force that avoids tension in the 2D material. Once it is in liquid, we can transfer it in acetone that dissolves PMMA. Afterwards, we bring the sample back in isopropanol in the critical superdryer. It replaces isopropanol by liquid CO₂ and by overpassing the critical point, we have our sample in a gas phase medium without passing through a high surface-tension change of phases. These steps allow us to realize the structure on the figure 14 (c-d) where the WSSe is deposited on the substrate full of holes. This deposition technique creates membranes as the one that studied Anis Chiout and that we compared to the non-suspended 2D material.

We realized this whole transfer technique multiple times with MoS₂ in order to optimize the procedure. We were able to cover few microns holes with MoS₂ flakes. That is for now the maximum size of the membranes that we have. As we can see on the figure 14, there are multiple steps to process to the transfer of a 2D material. The one shown previously allows to put our sample on holes that are electrically connected through gold contacts.

4.6 Technique of transfer on heaters

We know that it is not possible to study the thermal conductivity of a material if we heat the whole Si or SiO₂ substrate. We need to put them on a substrate that can help to really observe the behavior of our material. We need to avoid dissipation of heat everywhere else than in our material. That is why, when we do measurements, we always put the cell under vacuum. The vacuum avoids air to dissipate the heat. Moreover, we can use a substrate that have a very low conductivity and conductance. The other solution is to suspend the 2D material as a bridge between two contacts. Always under vacuum, it would avoid all other dissipation than the ones inside the 2D material and at the contacts. With this technique, we saw that some heating of the device is possible (on the sample of MoSe₂ over the hole). The inconvenient of this technique is that the heating is not fully controlled and it is not very performant in electrical insulators. To counter this problem, we can use heaters. 2D materials are put directly on heaters. They can be partially suspended. It is possible to heat locally the 2D material. Since the resistance that heats up the sample is not the 2D material, the Joule effect remains comparable for the heaters. It will be possible to heat conductors as insulators.

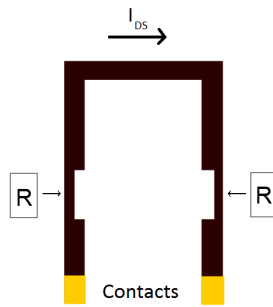


Figure 15: Schem of a loop of a heater.

The technique of transfers that we use contains multiple difficulties. The introduction of the water droplet may damage the 2D material and is not a solution that always works. Moreover, to melt the PMMA, a very high temperature is needed that is also a threat for our sample. In addition to that, the PMMA is not the part that we heat so the thermalization is not optimum. Some parts of PMMA may remain viscous. When we remove the bubble, this viscosity may be a problem because the 2D-material may be taken back by this viscous liquid. These problems are even more visible when we want to transfer our 2D material on a much

delicate substrate. That is for example the case of our heaters. They are composed of 2 suspended opened Si loops. The thickness of those suspended parts is of $4 \mu\text{m}$. On some parts of the loop, the width of Si is reduced. The width reduction acts as a resistance of about 500Ω each giving a whole resistance of roughly 1000Ω when we make a current pass through the loop. The place where the Si loop is open acts as contacts for electrical circuit. On the scheme 15, there is a representation of a heater loop.

The current heats up the Si principally between the two resistances. Having 2 different currents passing through the 2 loops allows us to obtain a specific temperature gradient if we are able to suspend a 2D material between both of them. The heaters are provided by Federico Panciera from the C2N laboratory. Since they are suspended and their dimensions are different from the one with the holes, modifications on the transfers are needed

To counter these problems, we used different ways. On exfoliated h-BN on SiO₂, we spincoated a layer of PMMA to protect the h-BN. Then, we put the sample 5 minutes in liquid nitrogen [22]. Because of the difference between the thermal expansion of SiO₂, h-BN and PMMA, the different materials move the one from each other. That increases the distance between the atoms that are bond. The bonds between SiO₂ and h-BN become lower. We dissolve PMMA in acetone to have only our 2D material on the sample. After nitrogen bath, when we want to pick up the flake by dry transfer, the use of the water droplet become unnecessary. Moreover, instead of PMMA, we tried to use another polymer (Polypropylene carbonate - PPC). This polymer has a lower glass temperature (45°C). The behavior of PPC is different than the one of PMMA because of it. We bring it to 39°C as PMMA before catching the h-BN. At 23°C , we move the PPC away from the SiO₂ and h-BN come with it. As say previously, there is a problem of thermalization of the polymer when we heat the sample. To limit this problem, we can take measure on the PDMS bubble that acts as a thermal reservoir. The air that thermalized better would be a more convenient stand to thermalize the PPC. In order to have air between PPC and PDMS, 2 changes are necessary. The first one is the change of the way to put PPC on PDMS. We used a tape with a hole at the center and we put it on a PPC spincoated layer. The PPC adheres to the tape and is taken even on the hole. After that, we just have to deposit the tape on PDMS. The second change that we need to do is to change the geometry of PDMS. For that, we make a cross opening inside our bubble and we separate our four parts of about 1 mm. In the middle of the bubble, there are no PDMS anymore and the thermalization of PPC is better. With this new setup, once we caught the 2D-material flake, we can deposit slowly the 2D material and PPC such that suspend them by putting the temperature between 65 and 85°C while touching both substrates. At this temperature, the PPC will melt on the substrate. H-BN is deposit with it. To even increase the attraction of the suspended structure, we functionalize the suspended bridge by using UV light. The transfer's station is in the laboratory only from a year. Because of that, the transfers are still to be optimize.

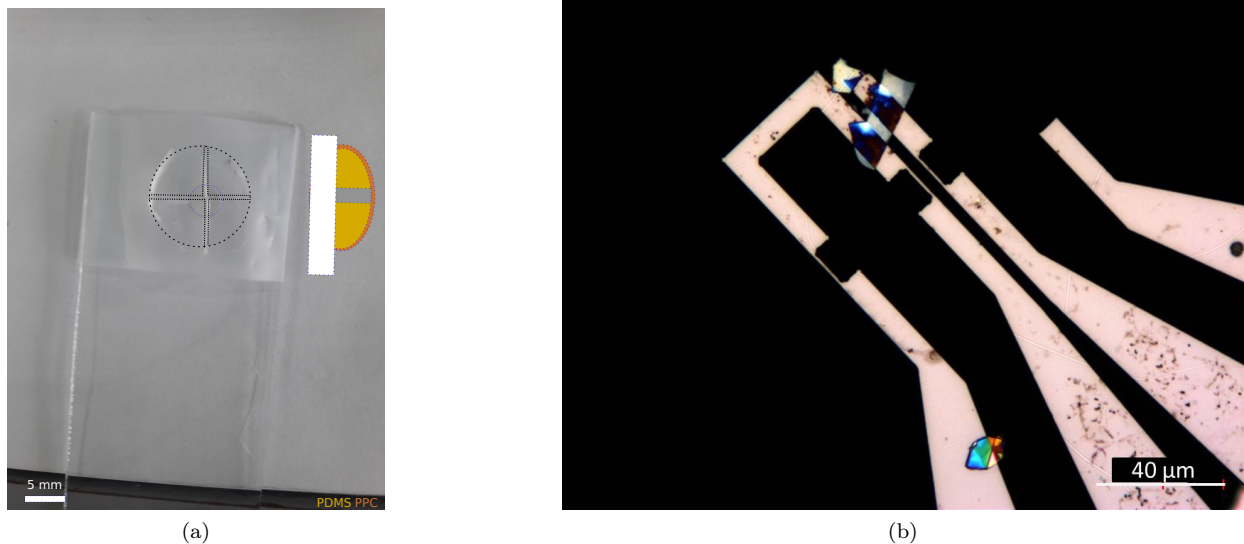


Figure 16: Upgrade procedure for the transfer of h-BN as suspended bridge on suspended loops. (a) Bubble of PDMS used to realize the transfer (b) Final sample after dissolution of PPC with h-BN forming a bridge between both loops.

On the photography 16 (a) , we see the PDMS bubble that was used to transfer h-BN on the suspended loop. The different parts of the bubble are highlighten by the dotted lines. The sheme of the bubble is shown near to the cross. The optical image 16 (b) is the heater after that the transfer was accomplished. It is composed of 2 loops and one of them is broken. h-BN is suspended between the both loops. It is freely suspended on 4.35 micrometers between the 2 loops. It is possible to heat the Si sample and the h-BN at the same time. On this heater, only the loop on the left can be heat since the second one is broken. However, it can still be useful to have a thermal gradient.

4.7 Thermal measurements on heaters

Once we have our 2D material on the heater, we can think of heating it. But first, we need to know how do the heater works. We need to calibrate the Raman peak position shift as function of the potential that is applied on the loop. For that, we use a cell that we put under vacuum inside which we calibrate our heater.

On the figure 17 (a), we plot the Raman spectra at 12 different applied voltages between 0 and 6 V. These spectra were taken on the loop between the resistances . The peak that we observe around 520 cm^{-1} is the peak characteristic of Si. We see that the position of the Raman peak decreases when the applied voltage increases. At $V = 6 \text{ V}$, the Raman peak is at 505 cm^{-1} . The total Raman shift is around 15 cm^{-1} that is quite important. This Raman shift can be attribute to the temperature rise by Joule effect. We can have access to the sample's temperature from the fact that the Raman peak shifts of $0.028 \text{ cm}^{-1}/\text{K}$ [7, 20]. On the figure 17 (b), we used both references to plot the temperature at the point where we took the Raman spectra as function of the applied power. We see that the heating is slow for voltage inferior to 2 V. Then, from this voltage, we have an increase of the heating. The maximum reached temperature is around $550 \text{ }^\circ\text{C}$ at 6 V. The figure 17 (c) is a map of the position of the Si peak when a voltage of 6 V is applied on the heater. We see that the Raman peak position and so the temperature are not at all homogeneous. On the broken heater, the Raman peak position is around 521 cm^{-1} . That corresponds to the peak position when the temperature is around 25°C . On the second heater on which is apply 6 V, we see that there are different areas. When we are close to the contact, the map is lemon yellow. It corresponds to a temperature around 200°C . When we are between the resistance, the position of the Raman shift decreases drastically near to

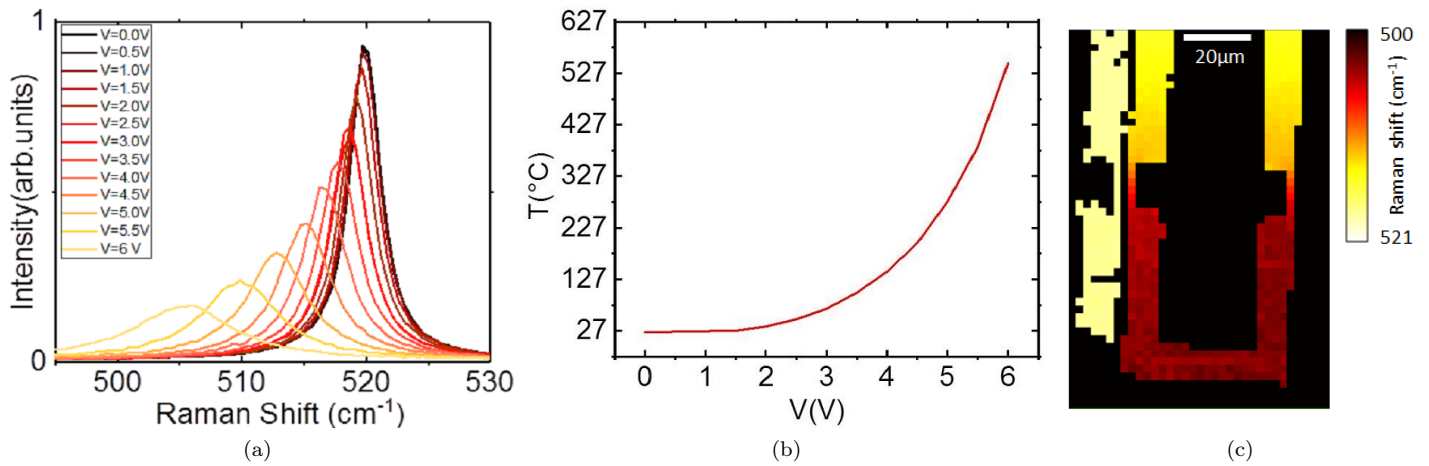


Figure 17: Calibration of the heater (a) Raman spectra at different VDS applied on the suspended part after the resistance. (b) Temperature variation when applied power increase. (c) Map of the position of the Si peak around 520 cm^{-1} with a laser at 532 nm .

502 cm^{-1} (in red wine on the map). That corresponds to a temperature around 600°C . As we can see, the temperature deviation is very high. We see that even if the second heater is at 600°C , the first one remains at a lower temperature. That is very interesting if we want to have a high temperature gradient. Indeed, the heat dissipation from one loop to the other is not effective.

Now that we checked how did the heater access to high temperature, we can work with structures on in.

We worked with flakes of InTe obtained from a crystal and exfoliated with commercial tape. Before suspending h-BN between the loops, we tried to use the heater to heat up a InTe stick that we deposited on the loop of the heater that works. With this setup, it was possible to heat InTe up to 250°C . This method is useful to avoid some stability problems that we can have with the Linkam cell that we used to calibrate other samples (SO₄ for example). Indeed, with this heating technique, the temperature was more precise and the thermalization stable. That avoid some defocusing effects that we can have with the Linkam cell that regulate the temperature by adjusting the resistance and the quantity of liquid nitrogen at each instant. The time variation of the resistance still needs to be analysed but this method is for sure usable.

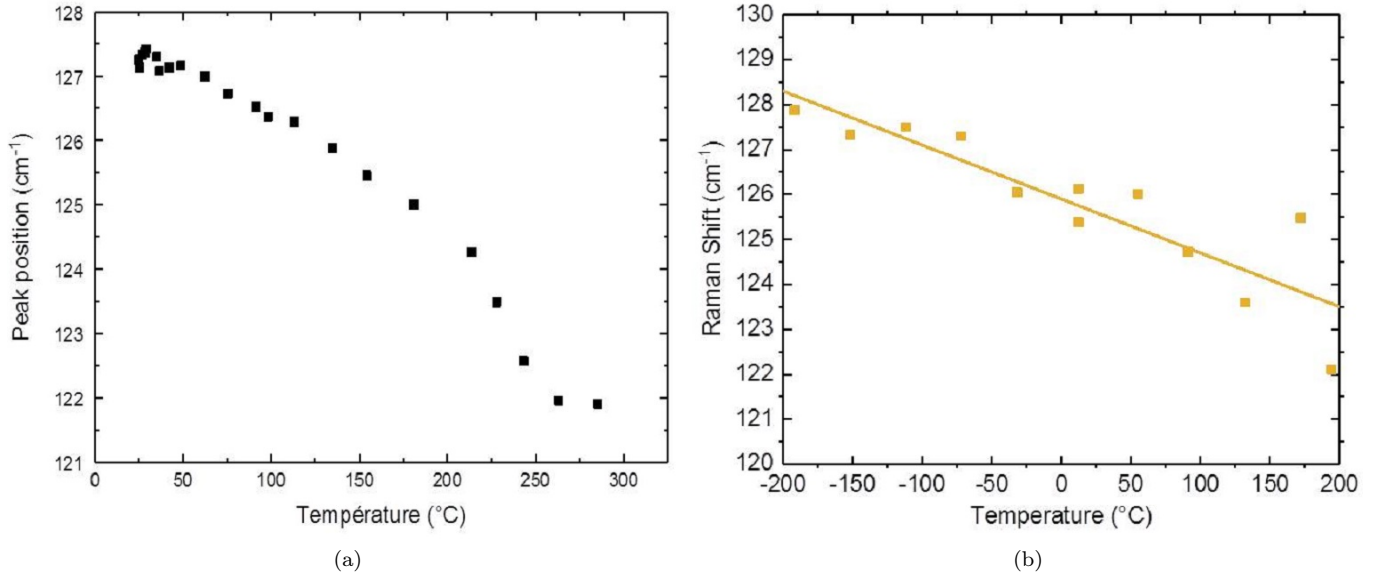


Figure 18: Raman shift of the position of InTe with a laser at 532 nm (a) on heater (b) inside the Linkam cell.

On the figure 18 (a), we see the variation of the main Raman peak position of InTe A_{1g} when we used the Si loop to heat the sample. On this graph, we see that there are different regimes of variation of the Raman shift position. From 22°C to 200°C , the decrease is linear with a slope of $-0,015 \pm 0,001 \text{ cm}^{-1}/\text{K}$. Then, from 200°C to 260°C , there are another linear decrease but with a higher slope of $-0,047 \pm 0,005 \text{ cm}^{-1}/\text{K}$. After this temperature a new regime appears till we burn the InTe and that the Raman peak are not visible anymore. We don't know what happened around 200°C and further experiments on it would be interesting. We can compare the figure 18 (a) with the figure 18 (b). On the figure 18 (b), we calibrated the shift of the Raman spectrum when we have a change of temperature in InTe in the Linkam cell to access another temperature range. For these measurements, we looked at the same peak as on the other spectrum. We did the measurements between -192°C and 177°C so that we didn't reached the second regime that appeared on figure 18 (a). In this case, the behavior that we see is more or less linear with a slope of $-0,012 \pm 0,002 \text{ cm}^{-1}/\text{K}$. It would be of interest to try to increase the temperature over 200°C to see if we find out the same variation of regime when we overpass 200°C .

The slopes obtained under 200°C are comparable and the mismatch may arise from the fact that we used 2 sticks of InTe. Theirs dimensions were a bit different and that can influence the heating. Both cells have advantages and inconveniats and it would be interesting to use both cells at the same time. We could put the whole sample at -192°C with the Linkam cell. At this temperature, it would be interesting to apply a voltage on the contacts of the heaters as we did in the other cell that we had. We can increase the temperature through the heaters. That allows to have an even higher gradient between the heater that is at high temperature and the one that is at low temperature. For the InTe, the measurement was only done as a calibration of the Raman shift as function of the temperature. It can afterward be used if we are able to suspend InTe on the heater. Nonetheless, the strange behavior around 200°C have to be further investigate.

5 Conclusion and perspectives

During this internship, we observed how a 2D material looks like when our point of interest are the optical phonons. We used a micro-Raman spectroscopy for this purpose. It allows us to determine the concentration in Se in $WS_{2x}Se_{2(1-x)}$ and the stress that we have in this material [10]. After that, we tried to heat up our samples using Joule effect. We did it with WSe_2 on h-BN and with MoS_2 suspended. We saw that for the non-suspended sample, we did not achieve to heat up the sample. For the suspended one, with the same power that we gave to our sample, the temperature increased. That means that suspended materials are maybe more interesting to study if we want to observe the thermal properties of our device. That constraints the device size and the way to construct them since it is not possible to suspend easily 2D materials. We achieved to suspend h-BN over $4.3 \mu\text{m}$ (figure 18). That is already interesting. There are now other transfers that we have to do. There are multiple techniques [22], [13]. But those techniques need to be optimized. The first main transfers are monolayer materials. With them, we can study the thermal conductivity of 2D materials. Then, we can realize heterostructures and see how do the thermal conductivity changes. Moreover, we can realize different shapes of devices to see how do the behavior change. Being able to suspend our material over higher sizes would be promising. Once we have the suspended 2D materials, we need to study their thermal conductivity. At this purpose, we can use the heaters provided by Federico Panciera. If we change the voltage that we apply on these heaters, it will be possible to heat the sample to 600°C . Moreover, we can even increase the gradient that we apply on our sample by putting it in the Linkam cell. There, it will be possible to decrease the temperature to -192°C . When we heat one part of the heater, it will be possible to have a temperature gradient. Very big gradient of temperature would be reachable. If we look at the theory in sample like that, it would be interesting to construct a model to describe this phenomena.

For now, we did few calibrations on the 2D materials that we want to study. We know that the peaks shifts with the temperature for MoS_2 and WSe_2 . Nonetheless, we still need to do some calibration on InTe since we detected a strange behavior around 200°C . We have to do a full measurement again from -192°C to 500°C . If we see also in this case a variation of the shift of InTe, it is possible that there is a new phase that appears at this temperature. It needs to be investigate. Nonetheless, for that, it is important that the Linkam cell remain stable in temperature. That is not the case for now since it is stable at low temperature but less when we heat the sample. We have to use a cooling system with water to stabilize our setup. Using the heaters, it could be interesting to see if the temperature gradient may induce a voltage gradient. If we were able to measure it somehow, we could have access to the Seebeck effect. This effect can be very interesting to generate a current from thermal gradient. The applications can be multiple. This effect is already used in Curiosity and Perseverance rovers that landed in Mars. But the applications can expand. For example, we could think about the water cooling systems that exist in thermal motors. In these systems, the water is hot. If we achieve to put a 2D material with a high Seebeck coefficient close to this temperature. And if we let it cold on the other side, it would be possible to create an electrical current that we could use. Moreover, 2D materials have captivating properties and there would be a great interest to use them more to replace old-fashioned materials.

References

- [1] B. Amin, T. P. Kaloni, and U. Schwingenschlögl. Strain engineering of ws₂, wse₂, and wte₂. *RSC Adv.*, 4:34561–34565, 2014.
- [2] Fugallo G. Paulatto L. et al. Cepellotti, A. Phonon hydrodynamics in two-dimensional materials. *Nat Commun*, 6400, 2015.
- [3] A. M. Dadgar, D. Scullion, K. Kang, D. Esposito, E. H. Yang, I. P. Herman, M. A. Pimenta, E.-J. G. Santos, and A. N. Pasupathy. Strain engineering and raman spectroscopy of monolayer transition metal dichalcogenides. *Chemistry of Materials*, 30(15):5148–5155, 2018.
- [4] Lukas Dobusch, Simone Schuler, Vasili Perebeinos, and Thomas Mueller. Thermal light emission from monolayer mos₂. *Advanced Materials*, 29(31):1701304, 2017.
- [5] Khalil L. Almabrouk H. et al. Ernandes, C. Indirect to direct band gap crossover in two-dimensional ws₂(1x)se₂x alloys. *npj 2D Mater Appl*, 5, 2021.
- [6] Giorgia Fugallo, Andrea Cepellotti, Lorenzo Paulatto, Michele Lazzeri, Nicola Marzari, and Francesco Mauri. Thermal conductivity of graphene and graphite: Collective excitations and mean free paths. *Nano Letters*, 14(11):6109–6114, 2014.
- [7] T. R. Hart, R. L. Aggarwal, and Benjamin Lax. Temperature dependence of raman scattering in silicon. *Phys. Rev. B*, 1:638–642, Jan 1970.
- [8] Yimo Han Hui Gao Saien Xie David A. Muller Jiwoong Park Kibum Kang, Kan-Heng Lee. Layer-by-layer assembly of two-dimensional materials into wafer-scale heterostructures. *Nature*, 550:229–233.
- [9] Nicholas Lanzillo, A. Birdwell, Matin Amani, Frank Crowne, Pankaj Shah, Sina Najmaei, Zheng Liu, Pulickel Ajayan, Jun Lou, Madan Dubey, Saroj Nayak, and Terrance O’Regan. Temperature-dependent phonon shifts in monolayer mos₂. *Applied Physics Letters*, 103, 07 2013.
- [10] Ahn-G. Shim J. et al. Lee, J. Optical separation of mechanical strain from charge doping in graphene. *Nat Commun*.
- [11] Broido-D. Esfarjani K. et al. Lee, S. Hydrodynamic phonon transport in suspended graphene. *Nat Commun*, 6290, 2015.
- [12] Wang-Y. Jiang J. et al. Li, Z. Temperature-dependent raman spectroscopy studies of 1–5-layer wse₂. *Nano Res.*, 13:591–595, 2020.
- [13] Xuezhi Ma, Qiushi Liu, Da Xu, Yangzhi Zhu, Sanggon Kim, Yongtao Cui, Lanlan Zhong, and Ming Liu. Capillary-force-assisted clean-stamp transfer of two-dimensional materials. *Nano Letters*, 17(11):6961–6967, 2017.
- [14] Nicolas Morell, Slaven Tepsic, Antoine Reserbat-Plantey, Andrea Cepellotti, Marco Manca, Itai Epstein, Andreas Isacson, Xavier Marie, Francesco Mauri, and Adrian Bachtold. Optomechanical measurement of thermal transport in two-dimensional mose₂ lattices. *Nano Letters*, 19(5):3143–3150, 2019.
- [15] Malic-E. Mueller, T. Exciton physics and device application of two-dimensional transition metal dichalcogenide semiconductors. *npj 2D Mater Appl*, 2, 2018.
- [16] Alessandro Principi, Mark B. Lundberg, Niels C. H. Hesp, Klaas-Jan Tielrooij, Frank H. L. Koppens, and Marco Polini. Super-planckian electron cooling in a van der waals stack. *Phys. Rev. Lett.*, 118:126804, Mar 2017.

- [17] Xin Qian, Jiawei Zhou, and Gang Chen. Phonon-engineered extreme thermal conductivity materials. *Nature Materials*, pages 1–15, 03 2021.
- [18] Zhehao Sun, Kunpeng Yuan, Zheng Chang, Shipeng Bi, Xiaoliang Zhang, and Dawei Tang. Ultra-low thermal conductivity and high thermoelectric performance of two-dimensional triphosphides (inp₃, gap₃, sbp₃ and snp₃): a comprehensive first-principles study. *Nanoscale*, 12:3330–3342, 2020.
- [19] Hesp N.C.H. Principi A. et al. Tielrooij, KJ. Out-of-plane heat transfer in van der waals stacks through electron–hyperbolic phonon coupling. *Nature Nanotech*, 13:41–46, 2018.
- [20] Raphael Tsu and Jesus Gonzalez Hernandez. Temperature dependence of silicon raman lines. *Applied Physics Letters*, 41(11):1016–1018, 1982.
- [21] Sam Vaziri, Eilam Yalon, Miguel Muñoz Rojo, Saurabh V. Suryavanshi, Huairuo Zhang, Connor J. McClellan, Connor S. Bailey, Kirby K. H. Smithe, Alexander J. Gabourie, Victoria Chen, Sanchit Deshmukh, Leonid Bendersky, Albert V. Davydov, and Eric Pop. Ultrahigh thermal isolation across heterogeneously layered two-dimensional materials. *Science Advances*, 5(8), 2019.
- [22] Peijian Wang, Shupeng Song, Arman Najafi, Chang Huai, Peihong Zhang, Yanglong Hou, Shaoming Huang, and Hao Zeng. High-fidelity transfer of chemical vapor deposition grown 2d transition metal dichalcogenides via substrate decoupling and polymer/small molecule composite. *ACS Nano*, 14(6):7370–7379, 2020.
- [23] Berthou S. Lu X. et al. Yang, W. A graphene zener–klein transistor cooled by a hyperbolic substrate. *Nature Nanotech*, 13:47–52, 2018.